http://dx.doi.org/10.5012/bkcs.2014.35.8.2295

Enhanced 2-Chorophenol Photodecomposition using Nano-Sized Mn-incorporated TiO_2 Powders Prepared by a Solvothermal Method

Dongjin Kim, Younghwan Im, Kyung Mi Jeong,[†] Sun-Min Park,[‡] Myeong-Heon Um,[§] and Misook Kang[*]

Department of Chemistry, College of Science, Yeungnam University, Gyeongsan, Gyeongbuk 712-749, Korea
[*]E-mail: mskang@ynu.ac.kr
[†]Department of Engineering in Energy and Applied Chemistry, Silla University, Sasang-gu, Busan 617-736, Korea
[‡]Korean Institutes of Ceramic Engineering and Technology (KICET), Geumcheong-gu, Seoul 153-801, Korea
[§]Division of Chemical Engineering, College of Engineering, Kongju National University, Cheonan 330-717, Korea
Received October 28, 2013, Accepted April 10, 2014

To effectively destruct 2-chlorophenol, a representative sterile preservative, nanometer-sized Mn (0.5, 1.0, 3.0 mol %)-incorporated TiO_2 powders were synthesized by a solvothermal method. XRD result demonstrated that the Mn ingredients were perfectly inserted into TiO_2 framework. The Mn-TiO_2 particles exhibited an anatase structure with a particle size of below 20 nm. The absorbance was shifted to the higher wavelength on Mn-TiO_2 compared to that of TiO_2. Otherwise, the PL intensities which has a close relationship for recombination between holes and electrons significantly decreased on Mn-TiO_2. The photodecomposition for 2-chlorophenol in a liquid system was enhanced over Mn-doped TiO_2 compared with pure TiO_2: 2-chlorophenol of 50 ppm was completely decomposed after 12 h when 1.0 mol % Mn- TiO_2 was used. Consequently, the core of this paper is as follows. introducing Mn into TiO_2 framework reduced the band-gap, moreover, it played as an electron capture resulted to lower recombination between electrons and holes during photocatalytic reaction for removal of 2-cholophenol.

Key Words : Mn-incorporated TiO_2, UV, PL, Destruction of 2-chlorophenol

Introduction

Many studies have been done on the photocatalytic treatment of environmental pollutants using semiconductors like TiO_2.[1,2] In particular, decomposing aromatic compounds with benzene ring has been attempted recently.[3,4] In general the removal of aromatic compounds is difficult in liquid photoreaction because of its super stability. 2-Chlorophenol, a representative sterile preservative, was selected by many researchers because it consists of double bonded carbons, chlorine, and hydroxyl groups. 2-Chlorophenol is widely used as a dye, an antiseptic, and is a precursor of polychlorophenol. However, it is poisonous, causing vomiting, inflammation in the digestive system, increased blood pressure, and convulsions when it absorbed through the skin and reaching the stomach through the circulation. In addition, when it attacks the skin, causing burns, it also can cause disturbances in the liver and kidney and is fatal at LD_{50} = 670 mg/kg. Thus more effective methods for 2-chlorophenol destruction are urgently required. Several researchers reported the treatment of wastewater containing 2-chlorophenol, examining the photocatalytic degradation of 2-chlorophenol by TiO_2.[5,6] However pure TiO_2 has a limitation for 2-chlorophenol degradation because of its long band-gap and rapid electron-hole recombination. Recent researches have focused on the metal oxides or sulfides doping/mixing to TiO_2 structure, such as ZnO,[7] SnO_2,[8] PtO,[9] ZnS,[10] or CdS,[11] which exhibit lower band gap energy. But, many metal-incorporated TiO_2s did not give better photo-activity, unfortunately. Some special researches also attempted the introduction of ozone or H_2O_2 during photo-catalysis to induce the higher oxidation to remove benzene derivatives difficult to decompose.[12,13] The results showed that the benzene derivatives photodecomposition was enhanced in the hybrid system. However, they rather cause secondary pollution. Therefore, efforts were made to come up with more stable photocatalysts with a higher oxidant property and good photoactivity. Here we tried to find high oxidizing ingredients, and realized that Fe, Cr, Mn, Os, or Ag is very good oxidizing metals. Generally an oxidizing agent transfers oxygen atoms to other materials, so the oxidizing agent can be called an oxygenation reagent or oxygen-atom transfer agent. Particularly, in the case of $[MnO_4]^-$, the oxides can also serve as electron acceptors, as illustrated by the conversion of $[MnO_4]^-$ to $[MnO_4]^{2-}$.

This present study, therefore, focused on the introduction Mn ingredient into TiO_2 framework to effectively decompose 2-chlorophenol. Mn-incorporated TiO_2 was synthesized using a solvothermal method, and was applied to photocatalytic decomposition of 2-chlorophenol. We discussed that the relationship between 2-chlorophenol photo-catalytic activity and the surface properties, and also mechanism of 2-chlorophenol photo-destruction.

Experimental

Synthesis of Mn-incorporated TiO_2. Mn-incorporated TiO_2 powders were prepared using a common solvothermal

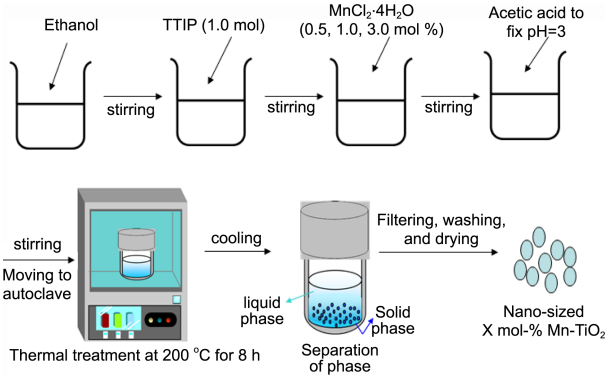

Figure 1. Procedure of Mn-incorporated TiO_2 using a solvothermal method.

method as shown in Figure 1. To prepare the sol mixture, mol titanium tetraisopropoxide (TTIP, 99.95%, Junsei Chemical, Tokyo, Japan) and manganese chloride ($MnCl_4$, 99.97%, Junsei Chemical) were used as the Ti and Mn precursors, respectively, with ethanol used as the solvent. Acetic acid was added to fix the pH = 3.0 after 1.0 mol TTIP and 0.5, 1.0, and 3.0 mol % Mn precursor added stepwise, and then homogeneously stirred. The final colloidal solution was moved to an autoclave. The TTIP and Mn chloride were hydrolyzed *via* the OR group during thermal treatment at 200 ºC for 8 h in an autoclave with 20 atm under nitrogen environment. The resulting precipitate was washed using distilled water until pH = 7.0, and then dried at 100 ºC for 24 h. Finally, the nano-sized Mn-TiO_2 powders were obtained.

Characterizations. The synthesized TiO_2 and 0.5, 1.0, and 3.0 mol % Mn-incorporated TiO_2 powders were identified using XRD (X'Pert Pro MPD PANalytical 2-circle diffractometer), nickel-filtered CuKα radiation (30 kV, 30 mA) at 2θ angles from 5 to 70º with a scan speed and time constant of $10^{o}min^{-1}$. The sizes and shapes of the TiO_2 and 0.5, 1.0, and 3.0 mol % Mn-incorporated TiO_2 were examined by TEM (JEOL 2000EX). UV-visible spectra of the TiO_2 and 0.5, 1.0, and 3.0 mol % Mn-incorporated TiO_2 powders were obtained using a Shimadzu MPS-2000 spectrometer (Kyoto, Japan) with a reflectance sphere. The spectral range was from 200 to 800 nm. The UV-visible absorption spectra of TiO_2 and 0.5, 1.0, and 3.0 mol % Mn-incorporated TiO_2 powders were obtained using a Cary 500 spectrometer with a reflectance sphere. Photoluminescence spectroscopy was conducted on the three powders to investigate photo-excited electron hole pairs using 1.0 mm thickness pellets of TiO_2 and 0.5, 1.0, and 3.0 mol % Mn-incorporated TiO_2 at room temperature using a He-Cd laser source at a wavelength of 325 nm.

Photo-Decomposition of 2-Chlorophenol. The decomposition of 2-chlorophenol was carried out using a bed photo reactors designed in the laboratory. 0.5 g Mn-TiO_2 powders were added into a qurtz cylinder reactor with 2.5 L volume including 2-chlorophenol aqueous solution of 1 L solution. The concentration of 2-chlorophenol was 50 ppm. UV-lamp (model BBL, 6 Wcm^{-2} × 3ea = 18 Wcm^{-2}, 30 cm length × 2.0 cm diameter; Shinan, Korea) with 365 nm was used as a light source. The 2-chlorophenol decomposition was done without air bubbling. Analyses of the concentration of 2-chlorophenol in the reaction solution before and after the reaction were done using UV-visible spectroscopy (Shimadzu MPS-2000 spectrometer).

Results and Discussion

Figure 2 shows the XRD patterns of TiO_2 and 0.5, 1.0, and 3.0 mol % Mn-TiO_2 powders, respectively. All of particles exhibited a pure anatase structure with peaks at 2θ values of 25.3, 38, 48.2, 54, 63, and 68º, which assigned to (101), (004), (200), (105), (211), and (204) diffraction planes, respectively.[14] Despite Mn ingredient was added into TiO_2 framework, the peak intensities were not changed and only slightly broaden. Additionally any peaks which attributed to the manganese oxide were observed. This result means that Mn ions were well inserted into the TiO_2 framework. It has been well established that peak broadening indicates a reduction in crystallite size.[15] Peak broadening of the 101 peak is related to the crystallite size of the hexagonal crystalline phase of anatase. Debye-Scherrer's equation, $t = 0.9\lambda/\beta\cos\theta$, where λ is the wavelength of incident X-rays, β is full width at half maximum height in radians, and the θ is the diffraction angle, was used to determine crystallite sizes.[16] On the basis of the full width at half maximum (FWHM) height of anatase peak at 2θ = 25.3º, those for TiO_2 and 0.5, 1.0, and 3.0 mol % Mn-TiO_2 were 19, 17, 14, and 13 nm, respectively.

Figure 3 presents TEM photographs of the particle shapes of TiO_2 and 0.5, 1.0, and 3.0 mol % Mn-TiO_2 particles. These were shown to consist of a relatively uniform mixture of spherical and rhombic particles with sizes of about 10-20 nm. When Mn components were added, the sizes were slightly decreased with Mn addition. The results showed the same tendency in XRD results.

Figure 4 exhibits the UV-visible spectra of TiO_2 and 0.5, 1.0, and 3.0 mol % Mn-TiO_2 particles. The absorption for

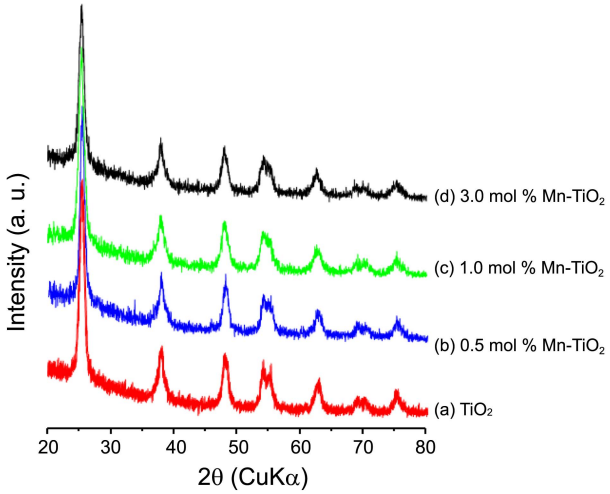

Figure 2. The XRD patterns TiO_2 and 0.5, 1.0, and 3.0 mol % Mn-TiO_2 particles.

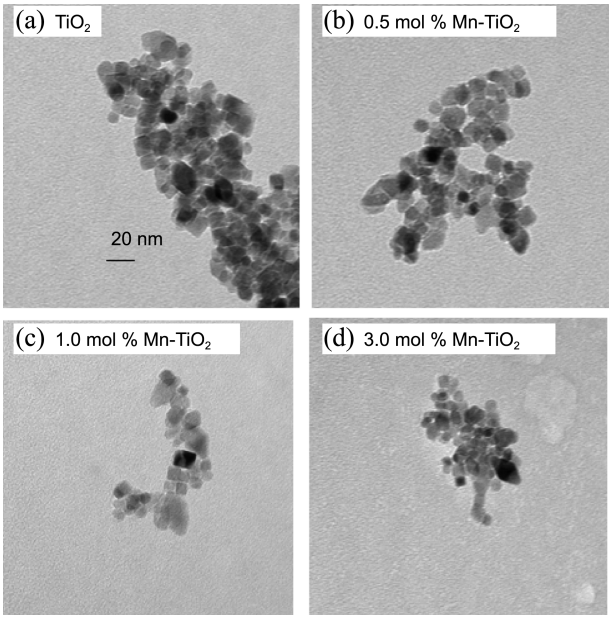

Figure 3. The TEM photographs of TiO_2 and 0.5, 1.0, and 3.0 mol % Mn-TiO_2 particles.

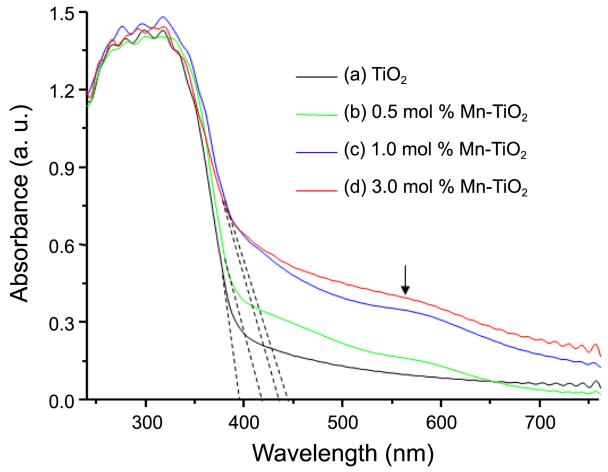

Figure 4. The UV-visible spectra of TiO_2 and 0.5, 1.0, and 3.0 mol % Mn-TiO_2 particles.

the six-coordination symmetry of Ti^{4+} normally appears around 350 nm.[17] When extrapolated, an absorption band was closed to 390 nm for pure TiO_2. In cases of the spectra for Mn-TiO_2, the absorption bands were shifted to higher wavelengths according to Mn concentration, and it was highest on 1.0 mol % Mn-TiO_2. Generally, the band gaps in a semiconductor material are closely related to the wave range absorbed. The higher the absorption wavelength, the shorter the band gap has. Using Tauc equation of $(\alpha h\nu)^n = B(h\nu - E_g)$,[18] their band-gaps were estimated to 3.18 (390 nm), 3.03 (410 nm), 2.96 (420 nm), and 2.92 (425 nm) eV for TiO_2 and 0.5, 1.0, and 3.0 mol % Mn-TiO_2 respectively. We postulate that the inserted Mn ingredients could change significantly the band gap energy of the TiO_2, leads to the efficient photocatalysis.

Figure 5 displays the PL spectra of TiO_2 and 0.5, 1.0, and 3.0 mol % Mn-TiO_2 particles. The PL curve means that the

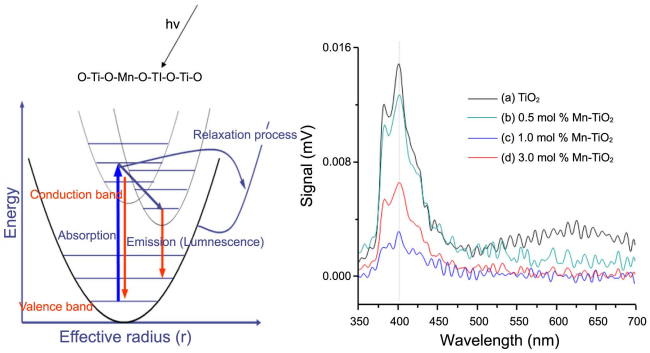

Figure 5. The PL spectroscopy of TiO_2 and 0.5, 1.0, and 3.0 mol % Mn-TiO_2 particles.

electrons in the valence band were transferred to the conduction band, after that the excited electrons were stabilized by photoemission. In general, the PL intensity increases with increasing number of emitted electrons resulting from recombination between excited electrons and holes, and a consequent decrease in photoactivity.[19] Therefore, there is a strong relationship between the PL intensity and photoactivity. The PL intensity decreases to a greater extent when a metal can capture excited electrons or exhibit conductivity, which is known as the relaxation process as shown in (a). The PL curves of the all samples exhibited the emission at 400 nm. The band broadening was attributed to the overlapped emission from the higher and lower excited states to the ground states. The PL intensity decreased significantly in the Mn-TiO_2, due to Mn captures photo-generated electrons from the TiO_2 conduction band, and thus, separates photo-generated electron-hole pairs. Thus, the presence of the Mn in TiO_2 framework reduces the recombination rate, and reduces PL spectrum intensity, indicating that PL intensity depends on electron capture by Mn.

Figure 6 gives the 2-chlorophenol removal over TiO_2 and Mn-TiO_2. Figure 6(a) showed a photo-reactor designed for 2-chlorophenol destruction in our laboratory. In initial step, the decomposed rate was the faster in 3.0 mol % Mn-incorporated TiO_2 compared with those of another catalysts. However after 8 h, the decomposition of 2-chlorophenol was enhanced in 1.0 mol % Mn-TiO_2. Additionally it, 2-chlorophenol of 50 ppm, was completely decomposed after 12 h, while the decomposition performance showed 80% in pure. Based on this result, it was concluded that the optimum Mn

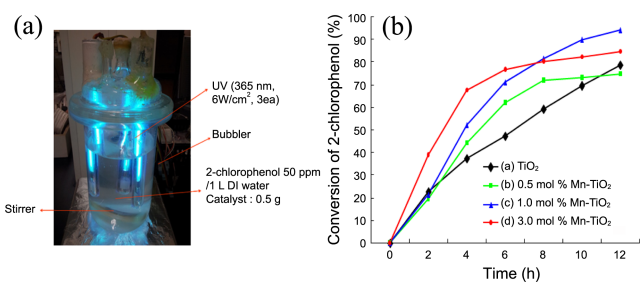

Figure 6. The photo-reactor (a) and 2-chlorophenol photodecomposition over TiO_2 and 0.5, 1.0, and 3.0 mol % Mn-TiO_2 photocatalysts (b).

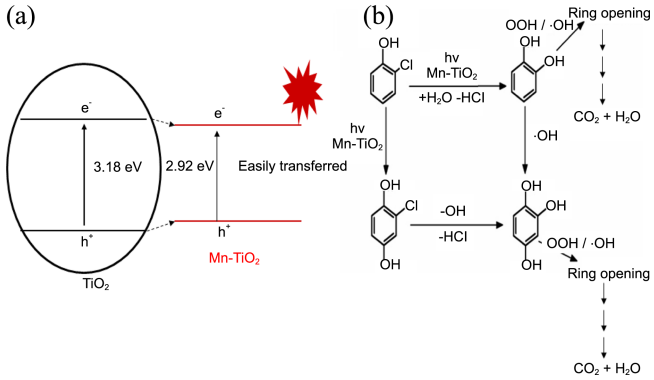

Figure 7. A band-gap model for Mn-TiO_2 (a) and a photocatalytic decomposition mechanism of 2-chlorophenol (b).

amount is 1.0 mol % for affectively 2-chlorophenol removal. The above results confirmed the importance of depressing recombination between electron and holes. The rate of photocatalytic degradation has been described by the Langmuir-Hinshelwood kinetic model, as shown in Eq. (1):

$$r = dC/dt = K_rK_aC/1 + K_aC \quad (1)$$

Where r is the rate of degradation, C the 2-chlorophenol concentration, t the time, K_r the reaction rate constant, and K_a the adsorption coefficient of 2-chlorophenol onto the photocatalyst particle. The equation can be simplified to a pseudo-first order equation, as presented in Eq. (2):

$$\ln (C_0/C_t) = K_rK_at = kt \quad (2)$$

Where C_0 is the initial concentration of 2-chlorophenol, C_t is the 2-chlorophenol at time t, and k is the apparent pseudo-first rate constant. A plot of $\ln(C_0/C_t)$ *vs.* time gives a linear relationship, the slope of which, upon linear regression, equals k. The order of the reaction constants were 7, 10, 11.67, and 17.5 $ppmh^{-1}$ until 4 h for TiO_2, 0.3 mol % Mn-TiO_2, 1.0 mol % Mn-TiO_2, 3.0 mol % Mn-TiO_2, respectively. This result indicated that the photocatalyst with higher electron attraction produced larger k values.

A band-gap model for Mn-TiO_2 photo-catalysis and a 2-chlorophenol photodecomposition mechanism are shown in Figure 7. In model (a), if the Mn ingredients are perfectly inserted into TiO_2 framework, the combination between TiO_2 and MnO_x gives the rapid initial photoreaction because of a shorter band gap, and thus raising the catalytic performance. Eventually The Mn-TiO_2 exhibited better catalytic performance than that of pure TiO_2. Here in (b), the decomposed steps for 2-chlorophenol were shown. The main suggested pathway for oxidation of 2-CP (chlorophenol) by OH radicals is represented. Due to the stronger *ortho/para* directory effect of OH-group than that of Cl-group, OH radical adds on the *ortho*/*para* position of OH– to form 2-chlorohydroxycyclohexadienyl ($C_6H_4(OH)_2Cl$) radicals. Then the Cl-position of 2-CP was replaced by OH to form dechlorinated aromatic product, hydroquinone. In the presence of O^{2-} on the conduction band of Mn-TiO_2, hydroquinone also could react with oxygen to form peroxyl radicals, leading to the opening aromatic ring and then form formic acid, acetic acid, oxalic acid, *etc.* eventually these are transferred to CO_2 and H_2O.

Conclusions

Through this study, we found out the effect of electron withdrawing metal ions in the framework TiO_2 photocatalyst on 2-chlorophenol removal. Three typed nano-sized Mn-incorporated TiO_2 powders were synthesized using a solvothermal method. The absorbance in Mn-TiO_2 shifted to the higher wavelength compared to pure TiO_2. The Mn-TiO_2 photocatalysts showed the lower PL intensity. The photodecompositions for 2-chlorophenol in liquid reaction were enhanced over Mn-TiO_2, in particular, 1.0 mol % Mn-TiO_2 completely decomposed 2-chlorophenol of 50 ppm after 12 h. From these results, we suggested that complete photooxidation for 2-chlorophenol dominated in Mn-TiO_2 than in pure TiO_2 and it depends on the electron accepting ability.

Acknowledgments. This research was financially supported by the Ministry of Education and National Research Foundation of Korea through the Human Resource Training Project for Regional Innovation (No. 2011 H1B8A2003313), for which the authors are very grateful.

References

1. Gupta, V. K.; Jain, R.; Mittal, A.; Saleh, T. A.; Nayak, A.; Agarwal, S.; Sikarwar, S. *Mater. Sci. Eng. C* **2012**, *32*, 12.
2. Liang, W.; Li, J.; Jin, Y. *Build. Environ.* **2012**, *51*, 345.
3. Selli, E.; Bianchi, C. L.; Pirola, C.; Cappelletti, G.; Ragaini, V. *J. Hazard. Mater.* **2008**, *153*, 1136.
4. Fabbri, D.; Bianco Prevot, A.; Zelano, V.; Ginepro, M.; Pramauro, E. *Chemosphere* **2008**, *71*, 59.
5. Ku, Y.; Leu, R.-M.; Lee, K.-C. *Water Res.* **1996**, *30*, 2569.
6. Ilisz, I.; Dombi, A.; Mogyorósi, K.; Farkas, A.; Dékány, I. *Appl. Catal. B* **2002**, *39*, 247.
7. Gaya, U. I.; Abdullah, A. H.; Zainal, Z.; Hussein, M. Z. *J. Hazard. Mater.* **2009**, *168*, 57.
8. Kong, J.-T.; Shi, S.-Y.; Zhu, X.-P.; Ni, J.-R. *J. Environ. Sci.* **2007**, *19*, 1380.
9. Maugans, C. B.; Akgerman, A. *Water Res.* **2003**, *37*, 319.
10. Sharma, M.; Jain, T.; Singh, S.; Pandey, O. P. *Solar Energy* **2012**, *86*, 626.
11. Wilson, W.; Manivannan, A.; Subramanian, V. R. *Appl. Catal. A* **2012**, *441-442*, 1.
12. Pulido Melián, E.; González Díaz, O.; Doña Rodríguez, J. M.; Araña, J.; Pérez Peña, *J. Appl. Catal. A* **2013**, *455*, 227.
13. Bertelli, M.; Selli, E. *J. Hazard Mater.* **2006**, *138*, 46.
14. Ivanda, M.; Musić, S.; Popović, S.; Gotić, M. *J. Mol. Struct.* **1999**, *480-481*, 645.
15. Kongsuebchart, W.; Praserthdam, P.; Panpranot, J.; Sirisuk, A.; Supphasrirongjaroen, P.; Satayaprasert, C. *J. Cryst. Growth* **2006**, *297*, 234.
16. Abbas, Z.; Holmberg, J. P.; Hellström, A. K.; Hagström, M.; Bergenholtz, J.; Hassellöv, M.; Ahlberg, E. *Colloid. Surf. A* **2011**, *384*, 254.
17. Gurkan, Y. Y.; Turkten, N.; Hatipoglu, A.; Cinar, Z. *Chem. Eng. J.* **2012**, *184*, 113.
18. Shaban, Y. A.; El Sayed, M. A.; El Maradny, A. A.; Al Farawati, R. Kh.; Al Zobidi, M. I. *Chemosphere* **2013**, *91*, 307.
19. Liu, B.; Zhao, X.; Zhao, Q.; He, X.; Feng, J. *J. Electron Spectrosc. Related Phenomena* **2005**, *148*, 158.